J Fluoresc (2014) 24:1225–1234
DOI 10.1007/s10895-014-1405-0

ORIGINAL PAPER

Spectroscopic and Molecular Modeling Based Approaches to Study on the Binding Behavior of DNA with a Copper (II) Complex

Fatemeh Vahdati Rad · Mohammad Reza Housaindokht · Razieh Jalal · Hossein Eshtiagh Hosseini · Asma Verdian Doghaei · Sadegh Sadeghi Goghari

Received: 17 February 2014 / Accepted: 19 May 2014 / Published online: 28 May 2014

Abstract Blocking the division of tumor cells by small-molecules is currently of great interest for the design of new antitumor drugs. The interaction of a new metal complex with DNA was investigated through several techniques. Absorption spectroscopy and gel electrophoresis studies on the interaction of the Cu-complex of $(2a\text{-}4mpyH)_2$ $[Cu(pyzdc)_2$ $(H_2O)_2].6$ H_2O with DNA have shown that this complex can bind to CT-DNA with binding constant 3.99×10^5 M^{-1}. The cyclic voltammetry (CV) responses of the metal complex in the presence of CT-DNA have shown that the metal complex can bind to CT-DNA through partial intercalation mode and this is consistent with molecular docking analysis, quenching process and thermal denaturation experiments. The cytotoxicity of this complex has been evaluated by MTT assay. The results of cell viability assay on DU145 cell line revealed that the metal complex had cytotoxic effects.

Keywords Calf thymus DNA · Cyclic voltammetery · DU145 cell line · Cytotoxic

Introduction

DNA is a fundamental cellular target; most chemicals induce their antitumor effects by interacting with DNA, thereby, blocking the division of tumor cells, which is the basis for the design of new antitumor drugs [1]. Generally, small molecules can interact with DNA through three non-covalent ways: (i) electrostatic interactions with the negative charged phosphate groups of nucleic acid; (ii) binding to the DNA helix via groove mode; and (iii) intercalation between the planar ligands intercalating into the adjacent stacked base pairs of native DNA [2]. Intercalation raises the vertical separation of adjacent base pairs and induces distortions in the sugar-phosphate backbone [3] whereas groove binders fit into the DNA minor groove leading to little perturbation in the DNA structure [4]. Groove binders are generally crescent-shaped molecules [5] that have a very high AT base-pair specificity [6].

Recently, dicarboxylic acids have been extensively used as one polydentate ligand involved in various reactions and complexes which have interesting properties in biological systems [7]. Copper is a biologically essential element [8] that plays a significant role in the endogenous oxidative DNA damage associated with aging and cancer [9]. Copper complexes are known to be extensively limited in terms of biological action. It has been approved that Copper accumulates in tumors due to selective permeability of the cancer cell membranes [10]. In recent years, many anticancer properties of dicarboxylic acid and pyridine—containing complexes have been studied [11, 12]. The molecular structure of bis(2-amino-4-methylpyridinium) transdiaquabis (pyrazine-2,3-dicarboxylato)-cuprate (II) hexahydrate complex is shown in Fig. 1. Here, we have studied the interaction of this metal complex with calf thymus DNA (CT-DNA), by UV-vis absorption, fluorescence spectroscopy, thermal denaturation and viscosity measurements using the DNA-ligand docking technique. Cyclic voltammetry and gel electrophoresis were subsequently used to study this interaction. Electrochemical investigations of DNA interactions with the ligand can provide a useful complement to the previously used methods of investigation, such as spectroscopic methods. Information obtained from our study would be helpful in finding the mode and the strength of

F. Vahdati Rad · M. R. Housaindokht (✉) · R. Jalal · H. Eshtiagh Hosseini · A. Verdian Doghaei · S. Sadeghi Goghari
Department of Chemistry, Faculty of Science, Ferdowsi University of Mashhad, Mashhad, Iran
e-mail: housain@um.ac.ir

M. R. Housaindokht · R. Jalal · H. Eshtiagh Hosseini
Research and Technology Center of Biomolecules, Faculty of Science, Ferdowsi University of Mashhad, Mashhad, Iran

the binding of the metal complex with DNA base pairs. We determined the binding constant (K_b) and the linear Stern-Volmer quenching constant (K_{sv}) for the interaction of the metal complex with CT-DNA by absorption and emission spectral studies. In addition, the cytotoxicity was determined by MTT (3-(4,5-dimethylthiazol-2-yl)2,5-diphenyltetrazolium bromide) assay on DU145 prostate cancer cell line.

Experimental

Materials and Methods

Calf thymus DNA was extracted from calf thymus tissue [13] and pcDNA3 was presented by the department of biology, faculty of science, Ferdowsi University of Mashhad. The $(2a\text{-}4mpyH)_2$ $[Cu(pyzdc)_2$ $(H_2o)_2].6$ H_2o metal complex was synthesized as we reported before [14]. All the experiments involving the interaction of the complex with CT-DNA were carried out in Tris-HCl buffer (0.01 M, pH=7.4). The supporting electrolyte was 50 mM NaCl/5 mM Tris HCl, pH=7.1. All solutions were prepared with doubly distilled water. The purity of the CT-DNA was investigated by taking the ratio of the absorbance values at 260 and 280 nm in the respective buffer, which was found to be 1.8, indicating that the DNA was sufficiently free of protein [15]. The DNA concentration per nucleotide was determined by absorption spectroscopy using the molar extinction coefficient value of 6,600 dm^3 mol^{-1} cm^{-1} at 260 nm [16]. The stock solution was stored at −20 ˚C. Penicillin/Streptomycin, Trypsin-EDTA, FBS, RPMI were obtained from Biosera. MTT was purchased from Sigma Chemical Company. Cell lines of DU145 were obtained from National Institute of Genetic Engineering Tehran. The other chemicals used were obtained from Merck.

UV Spectroscopy Studies

UV-vis spectra were recorded on a Shimadzu UV-Vis 2,550 spectrophotometer. Absorption titration experiments were performed by a constant concentration of metal complex (15.47 μM) while gradually increasing the concentration of DNA (5.4–30.9 μM). In order to measure the absorption spectra, an equal amount of DNA was added to both the test solution and the reference solution to omit the absorbance of DNA itself.

Fluorescence Studies

In order to evaluate the interaction of DNA with the metal complex, the fluorescence titration was carried out. Fluorescence spectra were recorded on Shimadzu RF-1,501 spectrofluorophotometer. Emission spectra were recorded with an excitation wavelength of 293 nm. Increasing amounts of DNA (0.77–13.6× 10^{-6} M) were added directly into the cell containing the metal complex solution (2.87×10^{-6} M). The solution in the cuvette was mixed before each scan. All measurements were performed at 298 K.

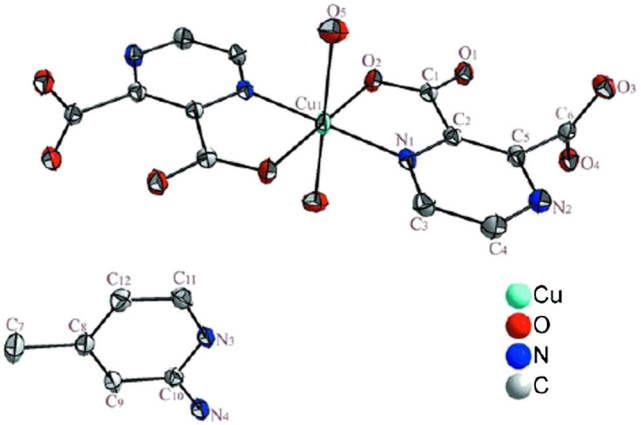

Fig. 1 The molecular structure of $(2a\text{-}4mpyH)_2$ $[Cu(pyzdc)_2$ $(H_2o)_2].6$ H_2o metal complex

Thermal Denaturation Studies

The studies on thermal denaturation were carried out with a Shimadzu UV-2,550 double beam spectrophotometer. The solution of the CT-DNA (60 μM) in 10 mM Tris-HCl buffer, pH=7.4, in the absence and presence of the metal complex (66 μM) was continuously heated, while the change of absorbance in the wavelength of 260 nm was monitored from 25 to 85˚C.

Viscosity Studies

For further identification of the binding mode, viscosity measurements can be done [17], whereas hydrodynamic measurements (e.g. viscosity and sedimentation) as the most essential tests of a binding model in solution, which are susceptible to the length change, are intended [18]. The viscometer which had been immersed in a thermostatic bath maintained at 25 °C, was employed for viscosity measurements. Titrations were performed by adding the metal complex to CT-DNA in the Tris-HCl buffer (10 mM, pH=7.4). DNA concentration was kept constant (5.4 μM) and the concentration of the metal complex was changed from 0 to 35 μM. Flow time was measured with a digital stopwatch and for each sample, the measurement was made in triplicates and the average value of flow time was recorded. The relative viscosity of DNA in the presence and absence of the metal complex was calculated from the Eq. (1):

$$\frac{\eta}{\eta_0} = \frac{t}{t_0} \tag{1}$$

where, t_0 and t are the flow time observed in the absence and presence of metal complex. Plot is presented as η/η_0 versus 1/r

[19], where r = [DNA]/[complex] and η and η_0 are the relative viscosity of DNA in the presence and absence of metal complex, respectively.

Gel Electrophoresis Studies

To investigate the effect of the metal complex on the electrophoretic mobility of DNA, supercoiled pcDNA3 (600 ng) was incubated with a different concentration of the metal complex (0–180 μM) without addition of any reductant, for 1 h at room temperature. The samples were electrophoresed for 1.5 h at 90 V on 0.8 % agarose gel in 0.5x TBE (Tris-boric acid-EDTA) buffer. Then the gel was stained with ethidium bromide at a concentration of 0.5 μg/ml. The stained gel was illuminated under a UV lamp and was photographed.

Cyclic Voltammetry Studies

Cyclic voltammetric technique has been used to explore the DNA binding mode. Cyclic voltammetric measurements were carried out using a Drop Sens (μStat 400) Potentiostat/Galvanostat Analyzer. All voltammetric experiments were performed in the single compartment cells with a volume of 5 ml. The three electrode system consisted of an Ag/AgCl as the reference electrode, the glassy carbon electrode (GCE) as the working electrode and a platinum wire as the auxiliary electrode. The supporting electrolyte was 50 mM NaCl/5 mM Tris HCl buffer at pH=7.1. The reaction solutions were deoxygenated by purging with nitrogen gas for 15 min prior to measurements. All experiments were carried out at 25 ˚C. The redox behavior of Cu(II) complex in the absence and presence of CT-DNA was studied by means of cyclic voltammetery within the potential range of −0.4 V to 0.3 V; the scanning rate was 0.1 V s^{-1}. Also, voltammetric behavior of Cu(II) complex in the absence of CT-DNA was studied within the range of scanning rate ($20<v<100$ mV s^{-1}).

In Vitro Cytotoxicity Assay

DU145 prostate cancer cells were cultured as a monolayer at the Roswell park memorial institute (RPMI-1,640) medium (containing GlutaMAX™-1 with 25 mM 2-[4-(2-hydroxyethyl)-1-piperazine] ethanesulfonic acid), supplemented with 10 % heat-inactivated fetal bovine serum and 1 % penicillin (100 U/mL)/streptomycin (100 μg/mL). All cells were incubated at 37 °C in a CO_2 atmosphere humidified up to 5 %. After 48 h, the medium was removed and replaced with a fresh medium containing serial concentrations of the metal complex for 24 h. The cytotoxicity assay for complex was evaluated by the MTT reduction method. The cells were then analyzed by the addition of 20 μL of 5 mg/mL MTT in phosphate-buffered saline (PBS), in which (3-(4,5-Dimethylthiazol-2-yl)-2,5-diphenyl tetrazolium bromide (MTT) is a tetrazolium salt soluble in yellow water. A mitochondrial enzyme in living cells, succinate-dehydrogenase, cleaves the tetrazolium ring and converts the MTT to an insoluble purple formazan. Therefore, the amount of formazan produced is proportional to the number of viable cells [20]. The plates were incubated for 4 h at 37 °C. After removal of the supernatant (the media), DMSO (dimethylsulfoxide) (150 μL) was added to dissolve the formazan crystals. The absorbance was monitored at 570 nm using an enzyme-linked immunosorbent assay (ELISA) Microplate Reader, ELX800G of Bio-Tek Instruments Inc. Every test was made in triplicates.

Molecular Modeling Studies

Molecular docking is a widely used powerful technique for investigation of DNA-drug interactions [21–23]. In this article, we used this tool to investigate the metal complex interaction with DNA. In present study, we used automated docking using a Lamarckian genetic algorithm [24] as implemented in the Arguslab software package [25, 26]. After adding hydrogen atoms to the input DNA structure (PDB code: 1DSC), the DNA structure was divided into two parts; binding site and rigid base pairs. The binding site would contain cytosine 5 and 13 and guanine 4 and 12 base pairs. Other base pairs were found to belong to the inflexible part. In addition to the basic structure of DNA, the basic configuration of the ligand was also required. For this purpose, the ligand structure was optimized by quantum mechanics methods. Optimization was performed at the B3LYP/lanl2dz level of theory by Gaussian 09 program package. After this organization, docking was performed and the most stable configuration was chosen as input for investigation.

Results and Discussion

UV- Vis Absorbance Measurement

The interaction of the metal complex with CT-DNA has been studied with UV- Vis spectroscopy in order to identify the possible binding mode to CT-DNA and to determine the binding constant to CT-DNA (K_b). The absorption spectra of the metal complex in the absence and presence of CT-DNA have been shown in Fig. 2. The changes observed in the UV- Vis spectra of the metal complex, after mixing it with CT-DNA, suggest that the metal complex interacts with CT-DNA. Upon addition of the concentration of CT-DNA, the absorption band of complex at 224 nm exhibits hypochromism (a decrease in the absorption intensity). This result suggests that the metal complex is likely to bind to the DNA helix via intercalation and this binding mode is related to the planarity of the molecular structure [27]. The

binding constant K_b was estimated from Half-reciprocal Eq (2) [28],

$$\frac{[DNA]}{(\varepsilon_a-\varepsilon_f)}=\frac{[DNA]}{(\varepsilon_b-\varepsilon_f)}+\frac{1}{K_b(\varepsilon_b-\varepsilon_f)} \quad (2)$$

where ε_a is the apparent absorption coefficient corresponding to A_{obsd}/[Complex], ε_f and ε_b are the extinction coefficient of the free metal complex and the extinction coefficient of the metal complex when fully bound to DNA, respectively. [DNA] is the concentration of DNA in base pairs. According to the plot of [DNA]/(ε_a–ε_f) versus [DNA], K_b was calculated from the ratio of the slope to intercept. The metal complex's binding constant (K_b) for 224 nm has been determined from the plot of [DNA]/(ε_a–ε_f) versus [DNA] and is estimated to be 3.99×10^5 M^{-1} (Fig. 3). This value is larger than those of the DNA minor groove binding Ru(II) complexes (1.1×10^4–4.8×10^4 M^{-1}), but smaller than those observed for the DNA classical intercalator (10^7–10^9 M^{-1}) [29]. The results suggest that this metal complex binds to DNA via partial intercalative mode. Thus, the intrinsic binding constant is similar to partial intercalators such as platinum (II) complex containing an antiviral drug (7.2×10^5 M^{-1}) [30].

Fluorescence Measurement

The interaction of metal complex with DNA has been studied using the fluorescence titration. The fluorescent emission spectra of the metal complex in the absence and presence of different concentrations of DNA have been presented in Fig. 4. Under our experimental conditions, aqueous solution of the metal complex reflects broad fluorescence between 360 and 460 nm, with the maximum at around 405 nm when excited at 293 nm. The spectra display that addition of different concentrations of DNA results in a gradual decrease in the fluorescence intensity of complex without any perceptible shift in λ_{max} [31]. The emission intensity is decreased due to self-stacking of some free bases in the compound along DNA surface [32]. If the complex interacts with DNA through classical intercalation, the emission intensity increases as the complex gets into a hydrophobic environment inside DNA [33]. Therefore, it is suggested that the complex does not bind to DNA by a classical intercalative mode [34].

To examine the fluorescence quenching induced by DNA, the well-known Stern-Volmer equation (Eq. (3)) was employed:

$$\frac{F_0}{F}=1+K_{SV}[Q]=1+k_q\tau_0[Q] \quad (3)$$

where F_0 and F are the fluorescence intensities in the absence and presence of the quencher, respectively, K_{sv} is the Stern-Volmer quenching constant, k_q is the biomolecular quenching constant, [Q] is the concentration of the quencher (DNA) and τ_0 is the excited state lifetime of the

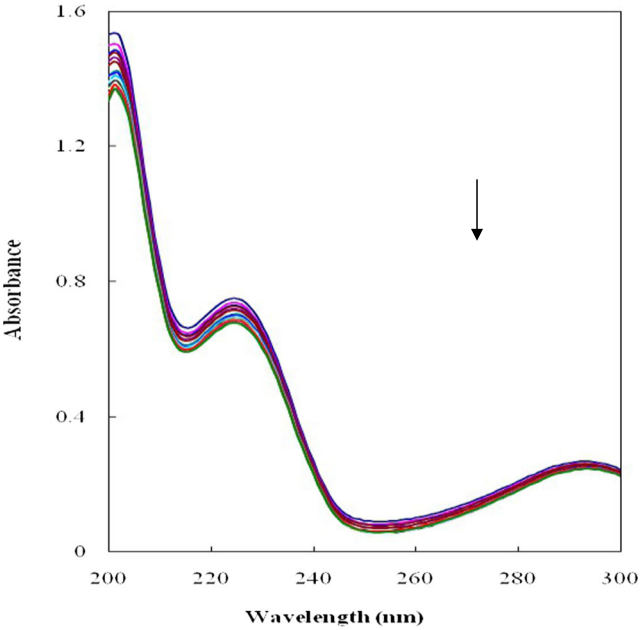

Fig. 2 The UV-vis absorption of the metal complex (15.47×10^{-6} M) in the absence and presence amounts of CT-DNA in Tris-HCl buffer (5.4–30.9)$\times10^{-6}$ M. Arrow shows the absorbance change upon the increase of CT-DNA concentrations. *T*=298 K, pH=7.4

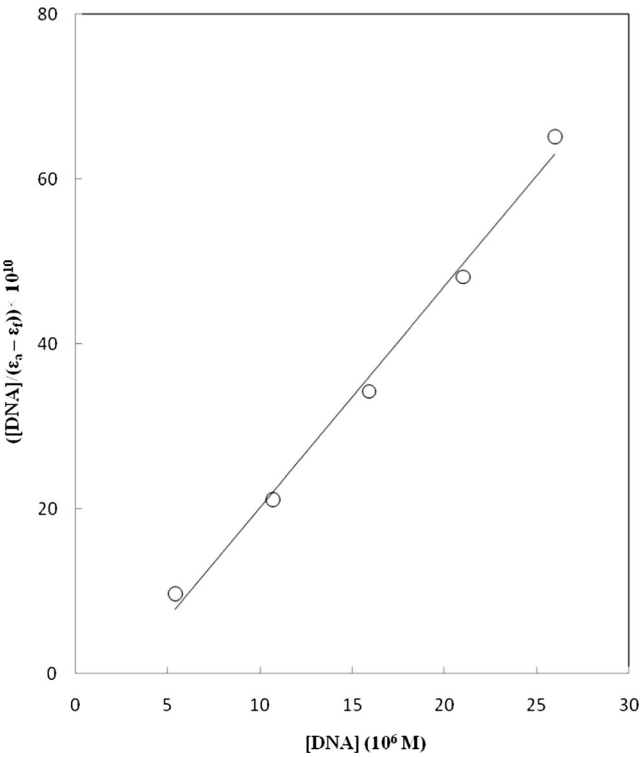

Fig. 3 Typical plot of [DNA]/(ε_a–ε_f) vs. [DNA] for absorption titration of increasing amounts of CT-DNA (5.4–30.9)$\times10^{-6}$ M with constant concentration of the metal complex (15.47×10^{-6} M) in Tris-HCl buffer at 224 nm; *T*=298 K, pH=7.4

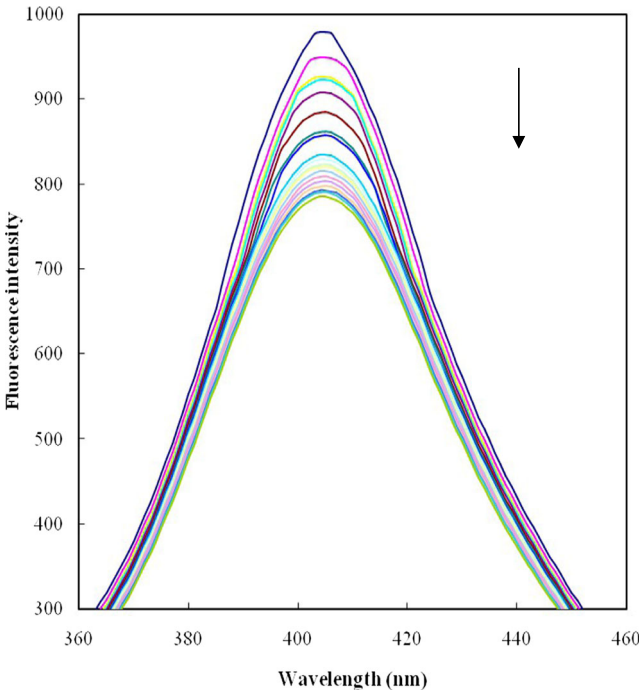

Fig. 4 Fluorescence emission spectra of the metal complex (2.87×10^{-6} M) in the absence and presence of CT-DNA ($0.77–13.6)\times10^{-6}$ M. Arrow shows the intensity changes upon increasing DNA concentrations; λ_{ex}=293 nm

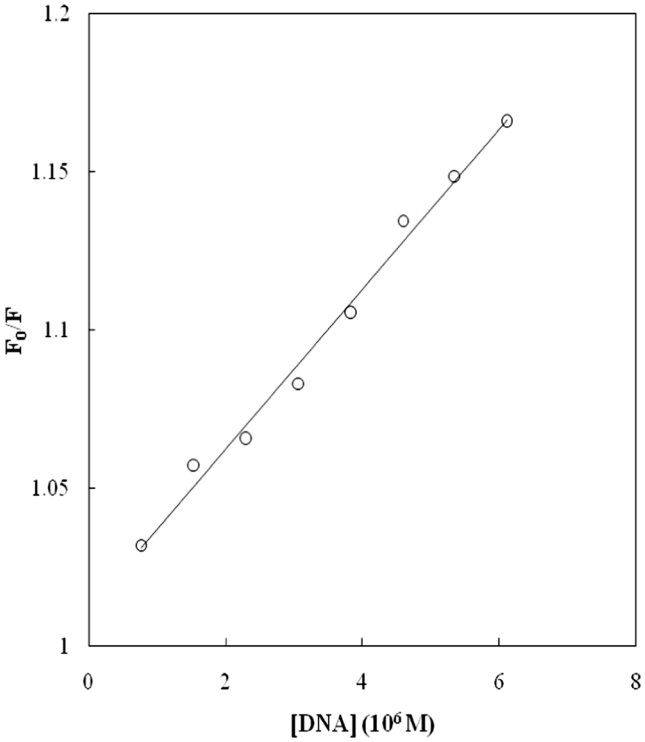

Fig. 5 Stern-Volmer plot the fluorescence quenching of the metal complex (2.87×10^{-6} M) by increasing amount of CT-DNA ($0.77–6.12)\times10^{-6}$ M at 298 K (λ_{ex}=293 nm, λ_{em}=405 nm)

biomolecule in the absence of the quencher ($\tau_0=10^{-8}$ s) [35, 36]. K_{sv} can be calculated through the slope of the Stern-Volmer plot (Fig. 5) which was estimated to be 2.53×10^4 M^{-1} and subsequently, $K_q = 2.53\times10^{12}$ L mol^{-1} s^{-1} was determined using the Eq (2). Since the obtained bimolecular quenching constant is greater than the largest possible constant in dynamic quenching (1.0×10^{10} M^{-1} s^{-1}), thus, the fluorescence quenching is not initiated here by a dynamic process, but instead by a static process that involves complex-DNA formation in the ground state [37]. The Stern-Volmer plot is linear, indicating that only one type of quenching process occurs [38, 39]. In order to obtain the binding constant for the interaction between the metal complex and DNA from the fluorescence quenching data, the Lineweaver-Burk equation (Eq. (4)) [40] was used:

$$\frac{1}{(F_0-F)} = \frac{1}{F_0} + \frac{1}{KF_0[Q]} \tag{4}$$

where F_0 and F are the fluorescence intensities of complex in the absence of DNA and at an intermediate concentration, respectively; K is the binding constant and [Q] is the quencher concentration. According to the slope of $1/(F_0–F)$ against 1/[Q], the binding constant was estimated to be 1.95×10^5 M^{-1} (Fig. 6).

Thermal Denaturation Measurement

The melting temperature (T_m) is the temperature at which the double stranded DNA denatures into single-stranded DNA [41]. Thermal denaturation of DNA is considered a method for the study of the stabilization/destabilization effect of ligands on DNA double helix [42]. The data were presented as A/A_0 versus temperature, where A and A_0 are the observed and the initial absorbance at 260 nm, respectively. The thermal denaturation curve for CT-DNA (60 μM) in the absence and presence of the metal complex (66 μM) was shown in Fig. 7. The presence of the metal complex retards the onset of denaturation temperature in DNA, indicating that there is an increase in stability of the double helical CT-DNA. Generally, this increase indicates that metal complex binds to DNA through intercalation mode, because intercalation of complex between DNA base pairs can lead to the stabilization of base stacking, thereby, increasing the melting temperature of double strand DNA [43].

Viscosity Measurements

Figure 8 shows that the viscosity of DNA solution decreases in the presence of the metal complex. This behavior suggests that the complex binds in a partial and/or non- classical

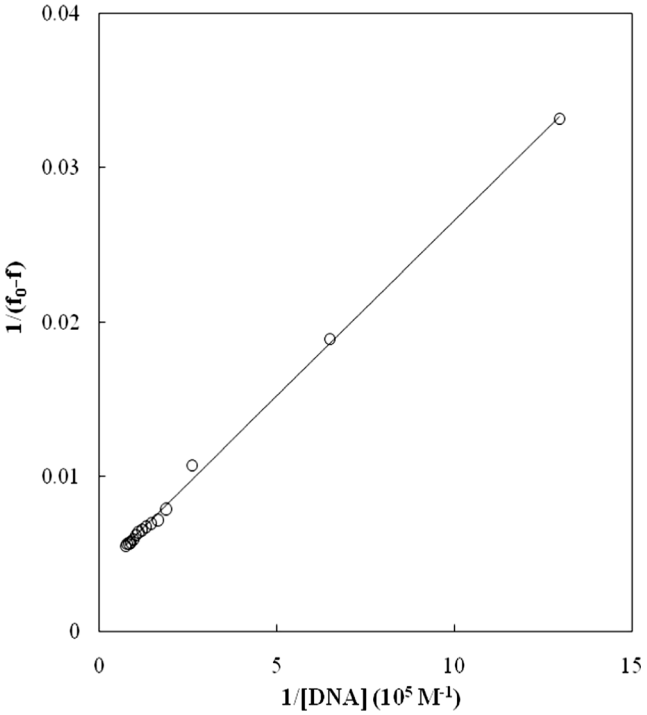

Fig. 6 The Lineweaver-Burk curve of the metal complex-CT-DNA at 298 K; The concentration of CT-DNA was (0.77–13.6) μM (λ_{ex}=293 nm, λ_{em}=405 nm)

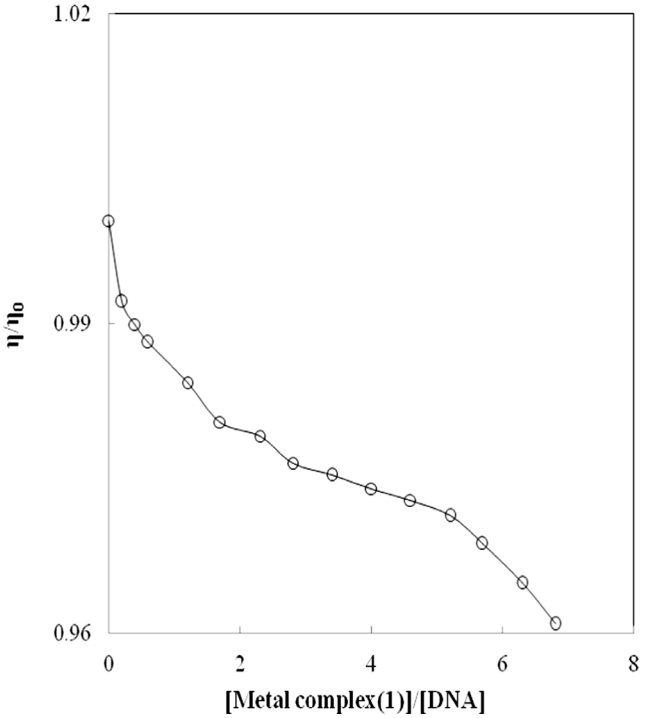

Fig. 8 Effect of increasing amounts of the metal complex (0–35 μM) on the relative viscosity of CT- DNA at 298 K. [DNA] =5.4×10^{-6} M

intercalation mode, which can bend the DNA helix and reduce its effective length and concomitantly its viscosity [44].

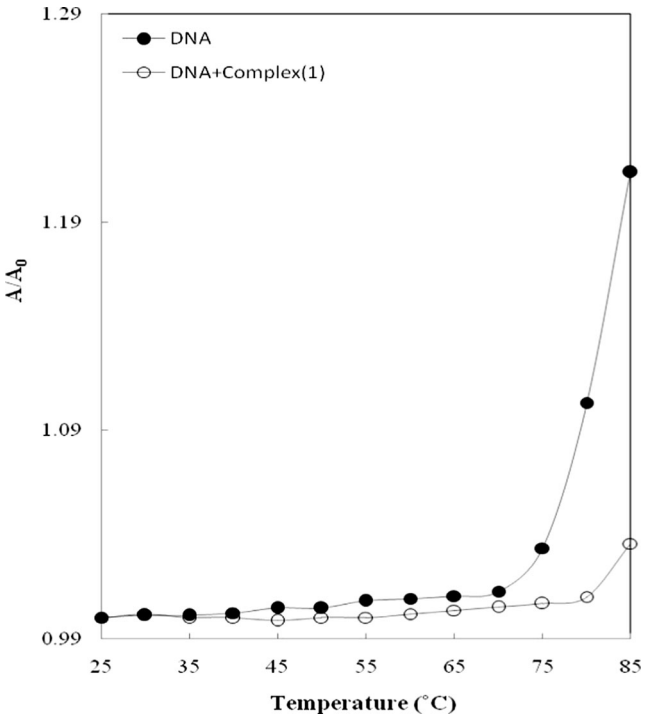

Fig. 7 Contrast curves of A/A_0 vs. temperature of CT-DNA (60×10^{-6} M) in the absence (solid circle) and presence (open circle) of the metal complex (66× 10^{-6} M)

Gel Electrophoresis Measurement

Lane 1 in Fig. 9 depicts the control DNA in the absence of the metal complex. This lane illustrates the presence of the open circular relaxed form (Form II), as well as the small amount of supercoiled form (Form I). Lanes 2–4 illustrate the increase in the concentration of metal complex (0–180 μM), leading to a decrease in the electrophoretic mobility of both DNA forms. Also, the amounts of supercoiled and open circular forms were not affected by the complex and hence it is approved that the metal complex has no nuclease activity. There are possible reasons for the decrease in the electrophoretic mobility of pcDNA3 in the presence of metal complex: (i) The metal complex binds to DNA which causes an increase in DNA molecular weight. (ii) The positive charges of the metal center may influence the net charge on the metal complex-DNA [45].

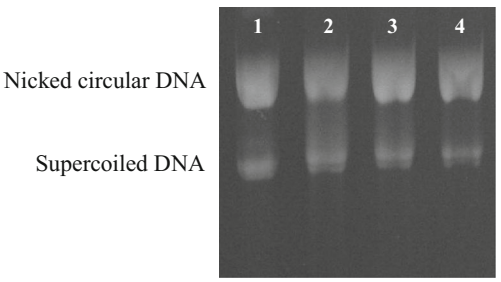

Fig. 9 Gel electrophoresis of pcDNA3 (600 ng) treated with the metal complex (1). Lane 1. control DNA, lane 2. DNA+80 μM (1), lane 3. DNA+120 μM (1), lane 4. DNA+180 μM (1)

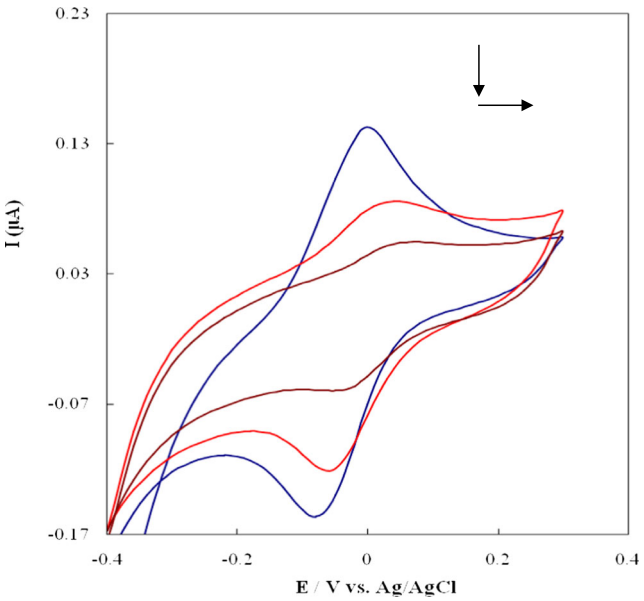

Fig. 10 Cyclic voltammograms of the metal complex (30.9×10^{-6} M) in the absence and presence of CT-DNA (14.6 and 29)$\times10^{-3}$ M in 50 mM NaCl/5 mM Tris-HCl, pH=7.1. Scan rates, 100 mV/s. Arrows show the drop of the voltammetric current and the peak potential shift upon the increase of CT-DNA concentrations

Cyclic Voltammetry

Figure 10 shows the cyclic voltammogram of metal complex (30.9 μM) in the absence and presence of CT-DNA (14.6 and 29) mM in 50 mM NaCl/5 mM Tris-HCl, pH=7.1 with 100 mV s^{-1} scan rate. The drop of the voltammetric currents in the presence of CT-DNA can be attributed to the diffusion of metal complex bound to the DNA molecule [46]. The peak potential shifts toward being more positive, indicating that the binding mode of the metal complex with DNA may be intercalation [47].

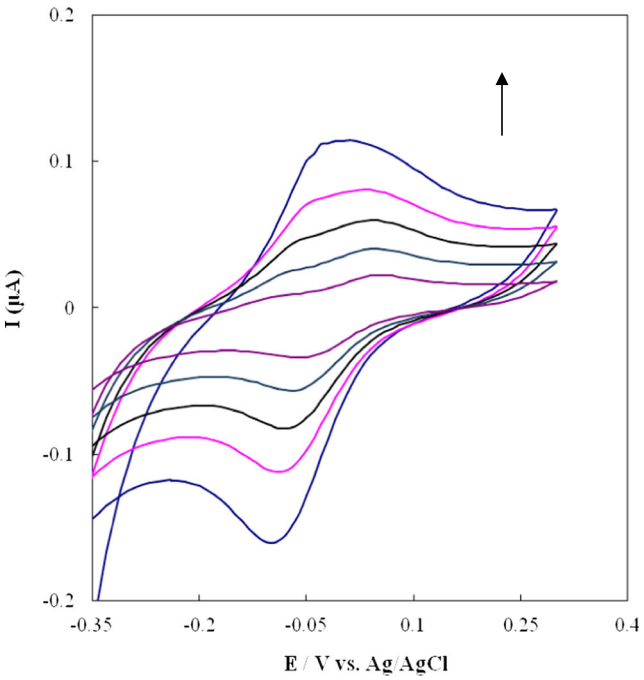

Fig. 11 Cyclic voltammograms of the metal complex (30.9×10^{-6} M) in 50 mM NaCl/5 mM Tris-HCl, pH=7.1. Scan rates 20, 40, 60, 80 and 100 mV/s

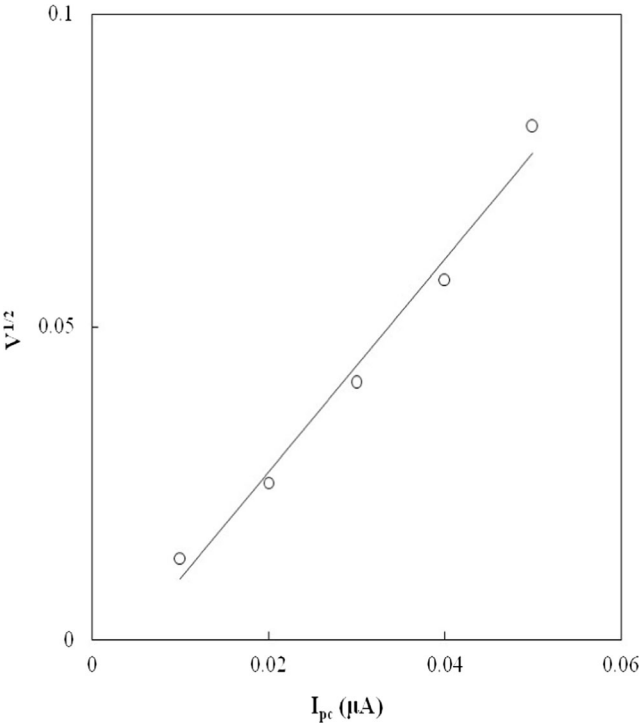

Fig. 12 The plot of the ipc. versus square root of scan rate for the metal complex (30.9×10^{-6} M)

Figure 11 shows the cyclic voltammogram of the metal complex (30.9 μM) in 50 mM NaCl/5 mM Tris-HCl, pH=7.1 and the range of scan rates (20–100 mV.s^{-1}). The Randles-Sevčik equation (Eq. (5)) predicts a linear relationship between the peak current and the square root of the scan rate:

$$i_p = \left(2.69\times10^5\right)n^{3/2}AD^{1/2}C\nu^{1/2} \quad (5)$$

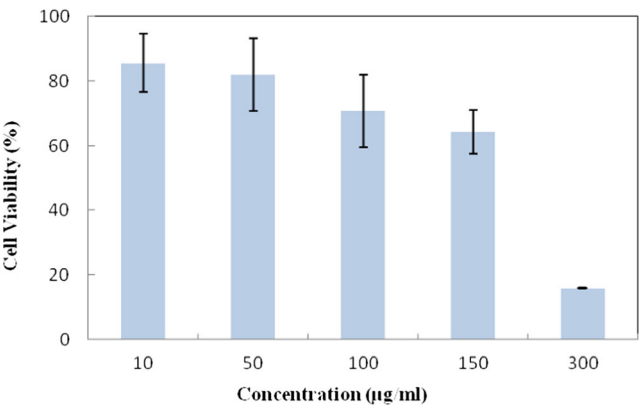

Fig. 13 Cell viability of the metal complex (10–300 μg/ml) on tumor DU145 cell proliferation in vitro over incubation periods of 24 h

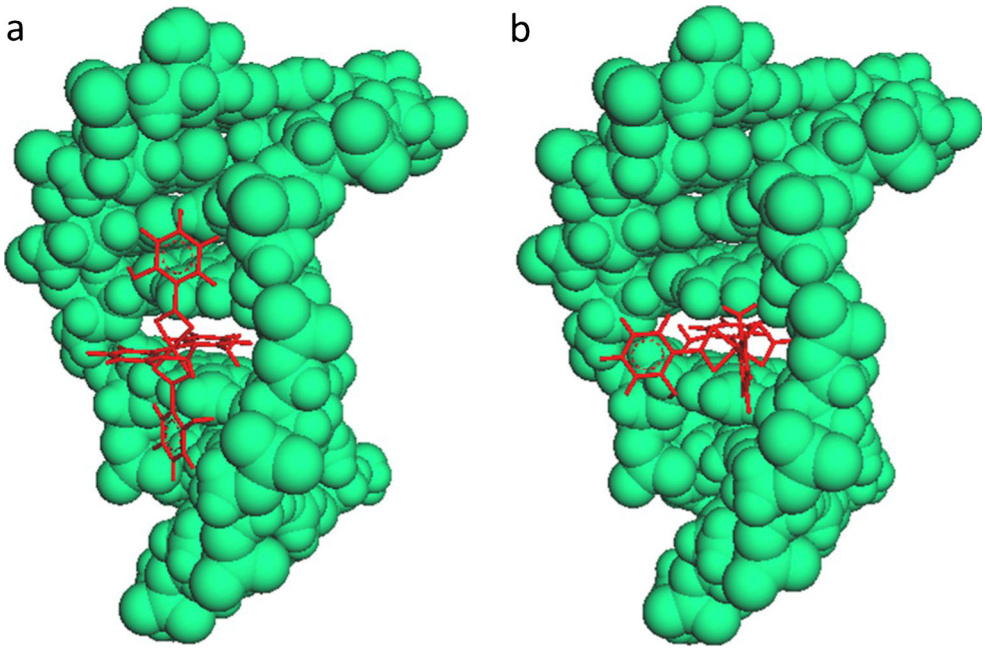

Fig. 14 Molecular docking of the metal complex of $(2a\text{-}4mpyH)_2[Cu(pyzdc)_2(H_2o)_2].6\ H_2o$ with DNA. Two stable docked structures, ligands are presented as cylinder and DNA is showed as CPK format. **a** Pyrimidine ring is located between base pairs with −4.26 kcal mol^{-1} energy. **b** Pyrimidine and phenol rings are placed between base pairs with −4.10 kcal mol^{-1} energy

where i_P is peak current (A), A surface area (cm^2) of the electrode, C bulk concentration (mol cm^{-3}) of electroactive species, D diffusion coefficient (cm^2/s) and υ scan rate (V/s) [48]. The linearity of the plot of square root of scan rate versus peak current (Fig. 12) and the values of i_{pa}/i_{pc} (=1) suggest that the redox tends to become reversible [49].

The separation between $E_b^{o'}$ and $E_f^{o'}$ can be used to determine the ratio of binding constants for the reduced and oxidized forms to DNA, using the Nernst equation (Eq. (6)) as follows [50]:

$$E_b^0 - E_f^0 = 0.059\log\left(K_{Cu(I)}/K_{Cu(II)}\right) \quad (6)$$

where $E^0{}_f$ and $E^0{}_b$ are the formal potentials of the Cu(II)/Cu(I) couple in the free and bound forms, respectively, and $K_{Cu(I)}$ and $K_{Cu(II)}$ are the binding constants of Cu(I) and Cu(II) forms to DNA, respectively. The ratio of constants for the binding of the Cu(I) and Cu(II) ions to DNA was estimated to be 3.22. This data suggests that the Cu(I) ion is apparently bound to DNA more strongly than Cu(II).

In Vitro Cytotoxicity Assay

Cancer is the third cause of death in Iran after coronary heart disease, accidents and other phenomena and prostate cancer is the third most common cancer among the males in Iran [51]. The cytotoxic effects of the metal complex was examined on cultured DU145 prostate cancer cells by exposing the cells for 24 h to a medium containing the metal complex at different concentrations (10–300 μg/ml). The complex inhibited the growth of the DU145 prostate cancer cells significantly in a concentration-dependent manner [52]. The cell viability decreased with addition of the different concentrations of complex [53]. The results obtained from the cell viability assay for different concentrations of metal complex against DU145 line cells with continuous exposure for 24 h are shown in Fig. 13. It is observed that metal complex shows cytotoxic activities in vitro probably due to the damage of DNA in cancer cells induced by the complex [54].

Molecular Modeling Studies

Molecular docking has been employed to reach an understanding of the interaction of metal complex and DNA. Based on our observations, the ligand can be intercalated in two stable modes within the structure of DNA. Figure 14 shows the details of two stable docked structures. As obvious in the form (**a**), the pyrimidine ring of the ligand is located between base pairs, while both the pyrimidine and phenol rings are placed in the form (**b**). Energy analysis shows that the form (**a**) is 0.16 kcal mol^{-1} more stable than form (**b**). This small difference in value indicates that both forms can exist. On the other hand, computations show that the ligand intercalates with DNA in two arrangements with almost same energy level.

Conclusions

In this study, we described DNA-binding properties of metal complex by UV-vis absorption, fluorescence spectroscopy, thermal denaturation, cyclic voltammetry and viscometry

measurements. Study of metal complex interaction with CT-DNA has been conducted using the fluorescence spectroscopy and gel electrophoresis and it reveals that metal complex can bind to CT-DNA. The emission spectra results showed that the intrinsic fluorescence of the metal complex was quenched through static quenching mechanism. UV-vis spectroscopic experiments have been used in order to determine the binding constant of metal complex to CT-DNA. The investigations on the metal complex interaction with CT-DNA show that the metal complex is capable of interacting with DNA through partial intercalation. The interaction occurrence is supported by the following findings:

(i) The value of K_b [in the range of 10^5 M^{-1}], the hypochromism of the UV-vis absorption band around 224 nm.
(ii) The positive shift of peak potentials along with peak currents decreases in cyclic voltammetry.
(iii) The decrease in viscosity of CT-DNA in the presence of metal complex. Also, the thermal denaturation studies and molecular docking analysis are in good agreement with cyclic voltammetry experiments. The results of cell viability assay on DU145 cell line revealed that the metal complex had cytotoxic effect in vitro, probably due to its binding to DNA. The present work may be helpful to the design of the new anticancer drugs.

Acknowledgments This research was supported by Ferdowsi University of Mashhad, Iran (Grant 3/21392-91/08/02).

References

1. Raman N, Selvan A (2011) DNA interaction, enhanced DNA photocleavage, electrochemistry, thermal investigation and biopotencial properties of new mixed-ligand complexes of Cu (II)/VO (IV) based on schiff bases. J Mol Struct 985:173–183
2. Ibrahim M, Shehatta I, Al-Nayeli A (2002) Voltammetric studies of the interaction of lumazine with cyclodextrins and DNA. J Pharm Biomed Anal 28:217–225
3. Gago F (1998) Stacking interactions and intercalative DNA binding. Methods 14:277–292
4. Chaires JB (1998) Drug—DNA interactions. Curr Opin Struct Biol 8: 314–320
5. Palchaudhuri R, Hergenrother PJ (2007) DNA as a target for anticancer compounds: methods to determine the mode of binding and the mechanism of action. Curr Opin Biotechnol 18:497–503
6. Wilson WD, Ratmeyer L, Zhao M et al (1993) The search for structure-specific nucleic acid-interactive drugs: effects of compound structure on RNA versus DNA interaction strength. Biochemistry 32: 4098–4104
7. Zhao B, Cheng P, Chen X et al (2004) Design and synthesis of 3d-4f metal-based zeolite-type materials with a 3D nanotubular structure encapsulated "water" pipe. J Am Chem Soc 126:3012–3013
8. Quan L, Sun T, Lin W, Guan X, Zheng M, Xie Z, Jing X (2014) BODIPY Fluorescent Chemosensor for Cu2+ detection and its applications in living cells: fast response and high sensitivity. J Fluoresc 1–6
9. Gao E-J, Lin L, Zhang Y et al (2011) Synthesis, characterization, and study on HeLa cells activity of a dinuclear complex [Cu < sub > 4</sub > (phen) < sub > 4</sub > (H < sub > 2</sub > O) < sub > 2</sub>] · (pyri) · 3H < sub > 2</sub > O. Eur J Med Chem 46:2546–2554
10. Arjmand F, Sayeed F, Muddassir M (2011) Synthesis of new chiral heterocyclic schiff base modulated Cu (II)/Zn (II) complexes: their comparative binding studies with CT-DNA, mononucleotides and cleavage activity. J Photochem Photobiol B Biol 103:166–179
11. Gao E-J, Sun T-D, Liu S-H et al (2010) Synthesis, characterization, interaction with DNA and cytotoxicity in vitro of novel pyridine complexes with Zn (II). Eur J Med Chem 45:4531–4538
12. Wang Q, Li W, Liu A et al (2011) Binding and photocleavage of a neutral nickel (II) bis (hydrogen pyridine-2, 6-dicarboxylato) complex to DNA. J Mol Struct 985:129–133
13. Janati Fard F, Mashhadi Khoshkhoo Z, Mirtabatabaei H et al (2012) Synthesis, characterization and interaction of < i > N</i > < i > N</i >'-dipyridoxyl (1, 4-butanediamine) Co (III) salen complex with DNA and HSA. Spectrochim Acta A Mol Biomol Spectrosc 97:74–82
14. Eshtiagh-Hosseini H, Gschwind F, Alfi N et al (2010) Bis (2-amino-4-methylpyridinium) trans-diaquabis (pyrazine-2, 3-dicarboxylato) cuprate (II) hexahydrate. Acta Crystallogr Sect E: Struct Rep Online 66:m826–m827
15. Psomas G (2008) Mononuclear metal complexes with ciprofloxacin: synthesis, characterization and DNA-binding properties. J Inorg Biochem 102:1798–1811
16. Carter MT, Rodriguez M, Bard AJ (1989) Voltammetric studies of the interaction of metal chelates with DNA. 2. Tris-chelated complexes of cobalt (III) and iron (II) with 1, 10-phenanthroline and 2, 2'-bipyridine. J Am Chem Soc 111:8901–8911
17. Lawrence D, Vaidyanathan V, Nair BU (2006) Synthesis, characterization and DNA binding studies of two mixed ligand complexes of ruthenium (II). J Inorg Biochem 100:1244–1251
18. Mitsopoulou CA, Dagas CE, Makedonas C (2008) Characterization and DNA interaction of the Pt (II) (pq) (bdt) complex: a theoretical and experimental research. Inorg Chim Acta 361:1973–1982
19. Grueso E, Prado-Gotor R (2010) Thermodynamic and structural study of pyrene-1-carboxaldehyde/DNA interactions by molecular spectroscopy: probing intercalation and binding properties. Chem Phys 373:186–192
20. Raja G, Butcher RJ, Jayabalakrishnan C (2012) Studies on synthesis, characterization, DNA interaction and cytotoxicity of ruthenium (II) schiff base complexes. Spectrochim Acta A Mol Biomol Spectrosc 94:210–215
21. Lengauer T, Rarey M (1996) Computational methods for biomolecular docking. Curr Opin Struct Biol 6:402–406
22. Ramalho TC, França TC, Cortopassi WA et al (2011) Topology and dynamics of the interaction between 5-nitroimidazole radiosensitizers and duplex DNA studied by a combination of docking, molecular dynamic simulations and NMR spectroscopy. J Mol Struct 992:65–71
23. Rohs R, Bloch I, Sklenar H et al (2005) Molecular flexibility in ab initio drug docking to DNA: binding-site and binding-mode transitions in all-atom Monte Carlo simulations. Nucleic Acids Res 33: 7048–7057
24. Morris GM, Goodsell DS, Halliday RS et al (1998) Automated docking using a Lamarckian genetic algorithm and an empirical binding free energy function. J Comput Chem 19:1639–1662
25. Thompson M (2004) Molecular docking using ArgusLab, an efficient shape-based search algorithm and the AScore scoring function. In: ACS meeting, Philadelphia
26. Thompson MA (2004) Molecular docking using ArgusLab, an efficient shape-based search algorithm and the AScore scoring function. In, ACS meeting, Philadelphia, 172, CINF 42

27. Ramachandran E, Kalaivani P, Prabhakaran R et al (2012) Synthesis, characterization, crystal structure and DNA binding studies of Pd (II) complexes containing thiosemicarbazone and triphenylphosphine/triphenylarsine. Inorg Chim Acta 385:94–99
28. Rajesh J, Gubendran A, Rajagopal G et al (2012) Synthesis, spectra and DNA interactions of certain mononuclear transition metal (II) complexes of macrocyclic tetraaza diacetyl curcumin ligand. J Mol Struct 1010:169–178
29. Pedras B, Batista RM, Tormo L et al (2012) Synthesis, characterization, photophysical studies and interaction with DNA of a new family of Ru (II) furyl-and thienyl-imidazo-phenanthroline polypyridyl complexes. Inorg Chim Acta 381:95–103
30. Shahabadi N, Moghadam NH (2012) DNA interaction studies of a platinum (II) complex containing an antiviral drug, ribavirin: the effect of metal on DNA binding. Spectrochim Acta A Mol Biomol Spectrosc
31. Krishna AG, Kumar DV, Khan B (1998) Taxol-DNA interactions: fluorescence and CD studies of DNA groove binding properties of taxol. Biochim Biophys Acta (BBA)-Gene Subj 1381:104–112
32. Nyarko E, Hanada N, Habib A et al (2004) Fluorescence and phosphorescence spectra of Au (III), Pt (II) and Pd (II) porphyrins with DNA at room temperature. Inorg Chim Acta 357:739–745
33. Song Y-F, Yang P (2001) Mononuclear tetrapyrido phenazine (tpphz) cobalt complex. Polyhedron 20:501–506
34. Zhou Q-H, Yang P (2005) Study on the binding mode of a Cu (II) complex with DNA. Acta Chim Sin 63:71–74
35. Lehrer S (1971) Solute perturbation of protein fluorescence. Quenching of the tryptophyl fluorescence of model compounds and of lysozyme by iodide ion. Biochemistry 10:3254–3263
36. Xu M, Ma Z-R, Huang L et al (2011) Spectroscopic studies on the interaction between Pr (III) complex of an ofloxacin derivative and bovine serum albumin or DNA. Spectrochim Acta A Mol Biomol Spectrosc 78:503–511
37. Ahmadi F, Alizadeh A, Shahabadi N et al (2011) Study binding of Al-curcumin complex to ds-DNA, monitoring by multispectroscopic and voltammetric techniques. Spectrochim Acta A Mol Biomol Spectrosc 79:1466–1474
38. Vaidyanathan VG, Nair BU (2003) Photooxidation of DNA by a cobalt (II) tridentate complex. J Inorg Biochem 94:121–126
39. Xu Z-H, Zhang X-W, Zhang W-Q et al (2011) Synthesis, characterization, DNA interaction and antibacterial activities of two tetranuclear cobalt (II) and nickel (II) complexes with salicylaldehyde 2-phenylquinoline-4-carboylhydrazone. Inorg Chem Commun 14:1569–1573
40. Zhang L, Xu J, Huang Y et al (2009) Enantioselective binding of l, d-phenylalanine to ct DNA. Spectrochim Acta A Mol Biomol Spectrosc 74:835–838
41. Mariappan M, Suenaga M, Mukhopadhyay A et al (2012) Synthesis, structure, DNA binding and photonuclease activity of a nickel (II) complex with a < i > N</i > < i > N</i >'-Bis (salicylidene)-9-(3, 4-diaminophenyl) acridine ligand. Inorg Chim Acta 390:95–104
42. Bahr M, Gabelica V, Granzhan A et al (2008) Selective recognition of pyrimidine-pyrimidine DNA mismatches by distance-constrained macrocyclic bis-intercalators. Nucleic Acids Res 36:5000–5012
43. Liu Y-J, Liang Z-H, Hong X-L et al (2012) Synthesis, characterization, cytotoxicity, apoptotic inducing activity, cellular uptake, interaction of DNA binding and antioxidant activity studies of ruthenium (II) complexes. Inorg Chim Acta 387:117–124
44. Satyanarayana S, Dabrowiak JC, Chaires JB (1992) Neither. DELTA.-nor. LAMBDA.-tris (phenanthroline) ruthenium (II) binds to DNA by classical intercalation. Biochemistry 31:9319–9324
45. Rajendran A, Magesh CJ, Perumal PT (2008) DNA-DNA cross-linking mediated by bifunctional [SalenAl< sup> III</sup>]< sup>+</sup> complex. Biochim Biophys Acta (BBA)-Gene Subj 1780:282–288
46. Zhang Q-L, Liu J-G, Liu J-Z et al (2002) Effect of intramolecular hydrogen-bond on the DNA-binding and photocleavage properties of polypyridyl cobalt (III) complexes. Inorg Chim Acta 339:34–40
47. Song Y, Yang P, Yang M et al (2003) Spectroscopic and voltammetric studies of the cobalt (II) complex of Morin bound to calf thymus DNA. Transit Met Chem 28:712–716
48. Grueso E, López-Pérez G, Castellano M et al (2012) Thermodynamic and structural study of phenanthroline derivative ruthenium complex/DNA interactions: Probing partial intercalation and binding properties. J Inorg Biochem 106:1–9
49. Mahadevan S, Palaniandavar M (1997) Spectroscopic and voltammetric studies of copper (II) complexes of bis (pyrid-2-yl)-di/trithia ligands bound to calf thymus DNA. Inorg Chim Acta 254:291–302
50. Jiang M, Li Y-T, Wu Z-Y et al (2009) Synthesis, crystal structure, cytotoxic activities and DNA-binding properties of new binuclear copper (II) complexes bridged by N, N'-bis (N-hydroxyethylaminoethyl) oxamide. J Inorg Biochem 103:833–844
51. Mousavi SM (2009) Toward prostate cancer early detection in Iran. Asian Pac J Cancer Prev 10:413–417
52. Kumar RS, Arunachalam S, Periasamy V et al (2009) Surfactant-cobalt (III) complexes: synthesis, critical micelle concentration (CMC) determination, DNA binding, antimicrobial and cytotoxicity studies. J Inorg Biochem 103:117–127
53. Huang H-L, Li Z-Z, Liang Z-H et al (2011) Synthesis, cellular uptake, apopotosis, cytotoxicity, cell cycle arrest, interaction with DNA and antioxidant activity of ruthenium (II) complexes. Eur J Med Chem 46:3282–3290
54. Wang H-F, Shen R, Tang N (2009) Synthesis and characterization of the Zn (II) and Cu (II) piperidinyl isoeuxanthone complexes: DNA-binding and cytotoxic activity. Eur J Med Chem 44:4509–4515